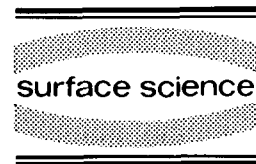




ELSEVIER

Surface Science 302 (1994) 49–56



# Monohydride structures on chemically prepared silicon surfaces

P. Jakob<sup>1</sup>, Y.J. Chabal<sup>\*</sup>, K. Kuhnke<sup>2</sup>, S.B. Christman

*AT&T Bell Laboratories, Murray Hill, NJ 07974, USA*

(Received 19 July 1993; accepted for publication 7 September 1993)

## Abstract

Chemically prepared, H-terminated silicon surfaces have been characterized by measuring their Si–H stretch infrared absorption spectra. This study focuses on two monohydride-terminated step structures present on stepped Si(111) surfaces with a  $\langle 11\bar{2} \rangle$  misorientation: the Si(111) $9^\circ\langle 11\bar{2} \rangle$  and the Si(110) surfaces. Analysis of the position and polarization of the observed vibrational bands shows that chemical etching promotes the formation of long rows of monohydride-terminated steps, with poor long range order in the direction perpendicular to the step edges. In particular, the chemically prepared H/Si(110) surfaces are atomically rough in one dimension while exhibiting atomically straight steps in the other.

## 1. Introduction

The observation that chemical etching of Si(111) surfaces in buffered HF solutions produces highly homogeneous, completely H-terminated H/Si(111)(1 × 1) surfaces [1], has stimulated a detailed characterization of these surfaces [2–7] to help understand the etching process. One of the remarkable results is that the contamination levels can be kept below 1% of a monolayer, even for surfaces with a large miscut with respect to the (111) direction [7].

The low contamination level has facilitated the study of the chemically prepared Si(111) $9^\circ$  sur-

faces misoriented in the  $\langle \bar{1}\bar{1}2 \rangle$  and  $\langle 11\bar{2} \rangle$  directions under various etching conditions (pH of the etching solution) [4]. The study of these vicinal surfaces with two and one dangling bonds, respectively, has been important to understand the kinetics and the chemistry of the etching process [5,6].

The etching process is highly anisotropic, with a faster attack of atomic defect and step kinks than of flat (111) planes. As a result, flat monohydride-terminated terraces are found on the vicinal (111) surfaces, separated by atomically straight double-layer steps [4,5]. Both dihydride- and monohydride-terminated steps or a mixture of both can be formed depending on the direction of misorientation. The dihydride-terminated steps have been studied more extensively so far because they involve an unusual strained local atomic structure which has presented some challenge to uncover [8].

\* Corresponding author.

<sup>1</sup> Present address: Physik Department E20, TU München, James-Frank-Strasse, 8046 Garching, Germany.

<sup>2</sup> Present address: Institut de Physique Experimentale, EPFL, Lausanne, Switzerland.

Studies of strongly misoriented Si(111) surfaces are relevant because they lead to the (311), (110) and (100) orientations for which etching is not well understood. The (110) plane corresponds to a  $35.3^\circ$  miscut of the (111) surface in the  $\langle 11\bar{2} \rangle$  direction while the (311) and (100) planes correspond to  $29.5^\circ$  and  $54.7^\circ$  miscuts of the (111) surface in the  $\langle \bar{1}\bar{1}2 \rangle$  direction, respectively. Since chemical etching of the Si(311) and Si(100) surfaces leads to a high degree of inhomogeneity [9], it is of particular interest to study the etching for miscuts in the  $\langle 11\bar{2} \rangle$  direction.

In this paper, we perform an infrared (IR) absorption study of the  $\text{Si}(111)9^\circ\langle 11\bar{2} \rangle$  and Si(110) surfaces. The Si(110) is chosen because the ideal surface is a perfect array of double-layer monohydride-terminated steps with the bulk unit cell periodicity ( $5.4 \text{ \AA}$ ) while the  $\text{Si}(111)9^\circ\langle 11\bar{2} \rangle$  has  $20 \text{ \AA}$  long (111) terraces between each double layer monohydride-terminated step. Unlike the dihydride type of steps, the monohydride steps are not subject to steric interactions, which may be the reason for their higher concentration on nominally flat Si(111) samples [6]. It is therefore expected that an ideal array of monohydride-terminated steps can be formed on the Si(110) surface by chemical etching.

## 2. Experimental

The chemical preparation of vicinal Si(111) has been described in detail in Refs. [4,5]. The etching speed depends on the pH and temperature of the HF solution. The higher the pH or the temperature of the solution, the faster the etching. The etching is also faster the higher the miscut from the (111) plane. The etching speed can be qualitatively monitored by noting the concentration of bubbles at the surface. In general, the conditions are set such that only a few bubbles can be seen on the surface by the end of the processing. For vicinal surfaces, this is usually achieved by lowering the pH from  $\text{pH} = 7.8$  of the 40%  $\text{NH}_4\text{F}$  solution by mixing it with buffered or pure HF. Occasionally, as noted in the figure captions, a lower temperature is used. The proportions used to produce the different pH solu-

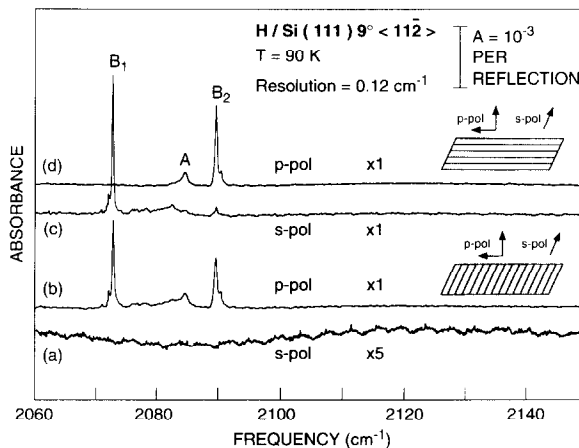


Fig. 1. Infrared absorption spectra of a chemically prepared  $\text{H}/\text{Si}(111)9^\circ\langle 11\bar{2} \rangle$  surface measured at  $T = 90 \text{ K}$  for two different orientations: spectra (a) and (b) are obtained with IR radiation propagating normal to the step edge, and spectra (c) and (d) with radiation propagating parallel to the step edge. The orientation of the electric field is indicated next to the sample schematics. Note that spectrum (a) is enlarged by a factor of 5.

tions are 1 part 49% HF and 100 parts 40%  $\text{NH}_4\text{F}$  for  $\text{pH} = 6.6$ , and 7:1 for the “buffered HF” of  $\text{pH} = 5.5$ .

All the IR absorption measurements are performed using multiple internal reflection as previously described [1,4,5]. The sample is maintained at low temperatures ( $85\text{--}90 \text{ K}$ ) during the measurements so as to minimize the thermal broadening [10]. The typical resolution is  $0.12 \text{ cm}^{-1}$  using a Happ–Genzel apodization. To achieve low temperatures without condensation on the surface, the samples are introduced into UHV using a clean load lock system [10].

## 3. Stepped Si(111) surfaces

### 3.1. Results

Fig. 1 shows a set of IR absorption spectra of  $\text{Si}(111)9^\circ\langle 11\bar{2} \rangle$  surfaces prepared by two minutes of etching in a  $\text{pH} = 6.6$  buffered HF solution at room temperature. A thermally grown oxide ( $\approx 1000 \text{ \AA}$  thick) is removed in HF prior to this etching step. The spectra are taken with p- and

s-polarizations for two different step orientations with respect to the IR radiation plane of incidence: for (a) and (b) the steps are orthogonal and for (c) and (d) the steps are parallel to the plane of incidence. Two polarizers are used for all four spectra to obtain 99% polarization efficiency (leakage below 1%).

The terrace monohydride mode (A) at  $2084.9\text{ cm}^{-1}$  is found to be substantially broadened as compared to the monohydride stretch mode at  $2085.9\text{ cm}^{-1}$  on the flat H/Si(111) surface. Both its width and its lower frequency are consistent with a wide distribution of small (111) domains on the stepped surfaces [11,12]. The sharpest modes,  $B_1$  at  $2072.69\text{ cm}^{-1}$  and  $B_2$  at  $2089.52\text{ cm}^{-1}$ , are attributed to Si–H monohydride species located at steps [4]. When the electric field is exactly along the step edge (curve a), no  $\nu_{\text{Si-H}}$  absorption bands can be detected in the range  $2060\text{--}2150\text{ cm}^{-1}$ . This observation indicates that the steps are atomically straight and that all step modes are polarized in the plane perpendicular to the step edge, just as is the case of the dihydride-terminated steps present on the  $\langle\bar{1}\bar{1}2\rangle$  mis-oriented Si(111) surfaces [4].

In Fig. 1, weaker features can also be observed: sharp shoulders on the sides of  $B_1$  and  $B_2$  and broader contributions in the spectral region between the  $B_1$  and the A modes ( $2072\text{--}2084\text{ cm}^{-1}$ ). These features reflect a modification of the local environment, due to an inhomogeneity in the direction perpendicular to the step edge as discussed below.

### 3.2. Discussion

Fig. 2 is a schematic drawing of the step structure with coupled monohydride termination. The orientation of the Si–H bond is parallel to the  $\langle 111 \rangle$  direction for the terrace silicon hydrides, including the last terrace row next to the step. The step Si–H species forms an angle of  $70.3^\circ$  relative to the  $\langle 111 \rangle$  axis. The vibrations of both the last terrace row and the step Si–H species are coupled together because the H atoms are bound to nearest neighbor silicon atoms. The resulting normal modes are the in-phase ( $B_2$ ) and out-of-phase ( $B_1$ ) motions of the two different type of

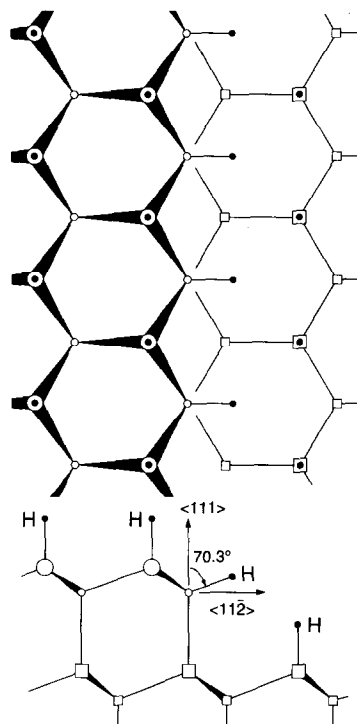


Fig. 2. Structure of the H/Si(111) $9^\circ\langle\bar{1}\bar{1}2\rangle$  surface showing the monohydride-terminated steps (note the zig-zag chain of coupled monohydrides formed by the first terrace row and the step H's). The crystallographic directions are indicated in the side view diagram.

hydrogens. According to geometrical considerations these symmetric ( $B_2$ ) and antisymmetric ( $B_1$ ) stretch modes are polarized in a plane perpendicular to the step edge, making angles of  $35^\circ$  and  $-55^\circ$  from the  $\langle 111 \rangle$  direction, respectively, that is  $26^\circ$  and  $-64^\circ$  from the surface normal.

Since only the monohydride and dihydride steps are observed upon chemical etching of a misoriented Si(111) surface [5,6], monohydride-terminated steps have dihydride-terminated kinks and vice-versa [13]. Therefore, the kink density of the monohydride-terminated steps in Fig. 1 can be estimated by analyzing the spectra in the region of the vibrational modes of the dihydride-step species. At 85 K, these modes have been observed [4,8] at  $2095.7\text{ cm}^{-1}$  ( $C_1$ ),  $2102.6\text{ cm}^{-1}$  ( $C_2$ ) and  $2135.8\text{ cm}^{-1}$  ( $C_3$ ). With the present experimental signal-to-noise ratio, the absence of any such feature in the data sets an upper limit of

1% for the kink density along the steps. That is the steps are atomically straight over distances longer than 300 Å.

The orientation of the dynamic dipoles associated with the  $B_1$  and the  $B_2$  step modes can be determined from the  $B_1$  and  $B_2$  intensities in the spectra of Figs. 1c and 1d. Using a screening factor of  $\epsilon_\infty = 1.8$  (Ref. [13]) and taking into account the field strengths  $E_{0i}$  ( $i = x, y, z$ ) in our particular detection geometry [4], the unscreened dipole moments of  $B_1$  and  $B_2$  are found to be inclined  $-74 \pm 3^\circ$  and  $20 \pm 1^\circ$ , respectively, with respect to the  $\langle 111 \rangle$  axis in the  $\langle 11\bar{2} \rangle$  direction, where the positive angles point towards the downward step direction. In this particular case the derived angles are rather insensitive to the value of  $\epsilon_\infty$  and a variation of  $\epsilon_\infty$  by 10% results in a shift of only  $1^\circ$ .

Clearly, the measured values ( $-74^\circ$  and  $+20^\circ$ ) are different from the theoretical predictions ( $-55^\circ$  and  $+35^\circ$ ). This discrepancy may be described as the observed perpendicular component of the  $B_1$  mode being smaller and that of  $B_2$  being larger than predicted. Qualitatively, the dynamical dipole coupling between the step and terrace monohydrides accounts for this observation. The excitation of the  $B_i$  modes leads to some excitation of the nearby terrace Si–H species. That is, the step modes are not entirely localized at the steps but extend into the terraces. The details of the coupling depend on the relative frequency of the step and terrace vibrations: for the  $B_1$  mode, the terrace and step Si–H's have out-of-phase motions because  $\Omega(B_1) < \Omega(A)$ , resulting in a lowering of the normal component of the dynamical moment of  $B_1$ ; for the  $B_2$  mode, the terrace and step Si–H's have in-phase motions because  $\Omega(B_2) > \Omega(A)$ , resulting in an enhancement of normal component of the dynamical moment of  $B_2$ .

## 4. The Si(110) surface

### 4.1. Results

Fig. 3 shows the infrared absorption spectra of a H/Si(110) surfaces etched in a mixture of 1

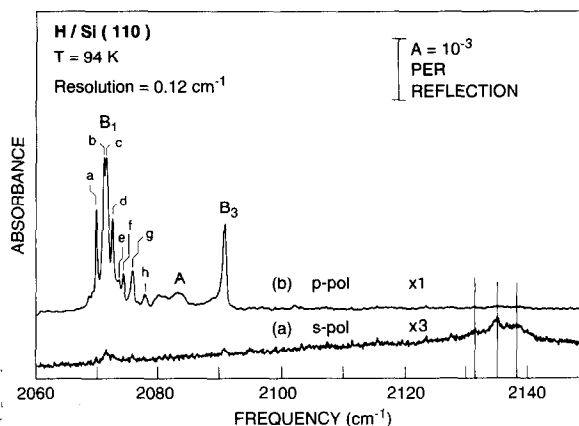


Fig. 3. Infrared absorption spectra of a chemically prepared H/Si(110) surface (pH = 5.5, 3 min etching at RT) measured at  $T = 94$  K. The IR radiation propagates normal to the step edge (s-polarization parallel to step edge). The spectrum using s-polarized light is enlarged by a factor of 3.

part HF 49% with 7 parts of  $\text{NH}_4\text{F}$  40% (pH  $\approx$  5.5) at room temperature. The curves (a) and (b) are obtained at a sample temperature of 94 K using s- and p-polarized radiation. The ideally H-terminated (110) surface would consist of rows of adjacent coupled monohydride steps. In Fig. 3, the geometry of the sample is such that these rows are oriented perpendicular to the IR beam plane of incidence, i.e., with the electric field of s-polarized radiation parallel to the step edges. The spectrum using p-polarized light (electric field perpendicular to both the surface plane and the step edges) shows a large number of vibrational bands in the monohydride region: a cluster labeled  $B_{1a-h}$  (2068–2078  $\text{cm}^{-1}$ ), another contribution labeled A (2080–2086  $\text{cm}^{-1}$ ) corresponding to terrace vibrations and a band labeled  $B_3$  ( $\sim 2091$   $\text{cm}^{-1}$ ). In the higher frequency part of the spectrum, there is only a very weak feature at 2103  $\text{cm}^{-1}$ . With s-polarized radiation, the only visible spectral features are at 2131.5, 2135 and 2138  $\text{cm}^{-1}$  (the weak bands at 2072 and 2091  $\text{cm}^{-1}$  are due to polarizer leakage).

As in the case of the H/Si(111) $9^\circ\langle 11\bar{2} \rangle$  surface (Fig. 1), all the step modes ( $B_{1i}$  and  $B_3$ ) and the A mode are polarized in the plane perpendicular to the step edge, i.e., the  $\langle 1\bar{1}0 \rangle$  direction. This observation indicates that the steps are atomically

straight over large distances (good long range order along the steps). Such homogeneity along the steps is confirmed by the narrow linewidths of the individual  $B_{1i}$  modes. The main source of inhomogeneity is the presence of dihydride-terminated kinks (involving the strained dihydride species), as evidenced by the broad band at 2130–2140  $\text{cm}^{-1}$  in s-polarization spectra [4,8]. This band is made up of a main peak at 2135  $\text{cm}^{-1}$  and two side bands at 2131.5 and 2138  $\text{cm}^{-1}$ . These side bands have been observed on the less homogeneous stepped Si(111) surfaces with a  $\langle\bar{1}\bar{1}2\rangle$  miscut [13], and assigned to the  $C_3$  mode of strained dihydrides located next to kinks. The relatively strong contribution of the side bands indicates that there are *short* dihydride-terminated steps on the H/Si(110) surface, consistent with the presence of kinks in monohydride-terminated steps.

#### 4.2. Discussion

The most striking feature of the spectra in Fig. 3 is the large number of sharp and discrete  $B_{1i}$  lines (arbitrarily labeled a–h in Fig. 3). Since each feature is narrow, the disorder along the steps is small: any such disorder would make the *average* terrace and step lengths apparently more continuous, resulting in broad instead of discrete, sharp features. The narrow widths therefore indicate that there is long-range order in one dimension. The number of discrete bands points to a structured disorder in the other direction. Such a structure probably is a consequence of the surface crystallinity where straight steps can only be separated by an integer number of rows in (111) terraces. The H/Si(110) surface is therefore not flat on the microscopic level, but rather involves a distribution of step–step distances. Two step–step interaction mechanisms that can contribute to the observed splittings, step–step dipole coupling and through-lattice strain, are considered next.

The frequency splittings due to dynamical dipole coupling between neighboring step and/or terrace Si–H species can be evaluated qualitatively [14,15]. Both parallel modes, such as the  $B_{1i}$ 's, and perpendicular modes, such as  $B_3$ , can be shifted by dipole coupling, although the mag-

nitude and sign of the shift depends on the relative orientations.

The dipole interaction matrix of two interacting dipoles ( $\mu_i$  and  $\mu_j$ ) can be written as:

$$I_{ij} = \text{const} \frac{e_i e_j - 3(e_i n_{ij})(e_j n_{ij})}{|\mathbf{R}_i - \mathbf{R}_j|^3}, \quad (1)$$

where  $e_i$  and  $e_j$  denote the unit vectors of two interacting dipoles  $\mu_i$  and  $\mu_j$  and  $n_{ij}$  is the unit vector of the spatial displacement  $\mathbf{R}_i - \mathbf{R}_j$ . If  $e_i$  and  $e_j$  are both perpendicular to  $n_{ij}$  the second term is zero and the expression simplifies to the more commonly used form  $I_{ij} = 1/|\mathbf{R}_i - \mathbf{R}_j|^3$ . This simplification applies for instance to a linear array of identical oscillators, i.e., to the various  $B_i$  and  $C_i$  step modes of slightly misoriented Si(111) samples, even though their polarizations are not perpendicular to the optical plane. For the H/Si(111)9° $\langle 11\bar{2} \rangle$  samples, the frequencies of both the  $B_1$  and the  $B_2$  modes are therefore blue shifted from those of an isolated monohydride species.

The situation, however, is more complex when another step row is placed in close proximity to the first row and the full expression must be used. In this expression, the second term counteracts the first, leading to different effects depending on the mode character. For example, for an array of monohydride steps, the  $B_1$  mode is red shifted while the  $B_2$  mode is blue shifted as a result of the step–step interaction. For an infinite array of dipoles parallel to the surface plane and arranged with a center of symmetry, there is no net shift because of opposing contributions from each side. The shift becomes non-zero for parallel dipoles if the number of interacting rows is finite, being largest for a single row.

On the Si(110) surface, there is a higher density of neighboring monohydride-terminated steps than on the H/Si(111)9° $\langle 11\bar{2} \rangle$  surface. The symmetric  $\nu_{\text{Si-H}}$  mode (labeled  $B_2$  for non interacting steps) should therefore be shifted due to step/step dipole interactions. The observation of the mode labeled  $B_3$ , with negligible contribution at the  $B_2$  frequency, is consistent with a high density of neighboring monohydride-terminated steps. This mode has a blue shift consistent with

the symmetric stretch dipole interaction of adjacent monohydride-terminated steps.

Dipole interactions do not account in detail for every measured feature. Although they give a qualitative understanding of the shifts, the largest possible shifts are of order  $2\text{ cm}^{-1}$  and cannot explain the position of all the  $B_{1i}$  lines in Fig. 3. Other effects, such as strain, should therefore also be considered. Strain of the Si backbonds and variations in the Si–Si–H bond angle probably affect the Si–H stretch frequency of the step hydrogen atoms. The strain induced frequency shifts, however, cannot be calculated using small cluster models and this issue has not yet been addressed with slab calculations. As a result, the interpretation remains speculative. If strain were the dominant mechanism for frequency shift, then our data would imply that the asymmetric  $\nu_{\text{Si-H}}$  mode ( $B_1$ ) is much more sensitive to strain than the symmetric one ( $B_3$ ).

## 5. Comparative studies

Fig. 4 shows Si–H stretch spectra of H-terminated silicon surfaces, with various miscuts and preparation conditions. The purpose is to compare and identify trends in the vibrational features in the region  $2060\text{--}2100\text{ cm}^{-1}$ , which are prominent in each spectrum and are indicative of the presence of coupled monohydride species. Curves (a) and (c) are identical to the spectra in Figs. 1b and 3b, taken from H/Si(111) $9^\circ\langle 11\bar{2}\rangle$  and H/Si(110) surfaces, respectively; curve (b) represents an enlarged ( $\times 5$ ) section of a spectrum of the H/Si(111) $9^\circ\langle \bar{1}\bar{1}\bar{2}\rangle$  prepared in a pH = 7.8  $\text{NH}_4\text{F}$  solution (Fig. 6 of Ref. [4]). The presence of coupled monohydride species on this last surface is attributed to faceting of the originally dihydride-stepped surface; the newly formed  $\langle 111\rangle$  facets are tilted by  $70.3^\circ$  relative to the original  $\langle 111\rangle$  plane and they are separated by monohydride-terminated steps. These are oriented at  $\pm 60^\circ$  from the original step edge and therefore correspond to extended kinks. As a result, the  $B_i$  related features are most prominent in s-polarization spectra, a sample of which is displayed in Fig. 4b.

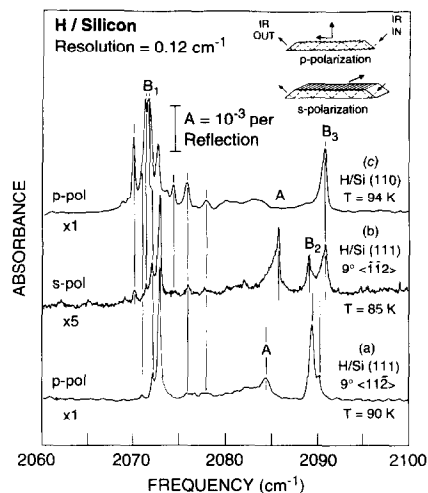


Fig. 4. Infrared absorption spectra of three chemically prepared H/Silicon surfaces: (a) H/Si(111) $9^\circ\langle 11\bar{2}\rangle$ , prepared at pH = 6.6 by 2 min etching at RT (measured at  $T = 90\text{ K}$ ); (b) H/Si(111) $9^\circ\langle \bar{1}\bar{1}\bar{2}\rangle$ , prepared at pH = 7.8 by 7 min etching at  $T \approx 273\text{ K}$  (measured at  $T = 85\text{ K}$ ); and (c) H/Si(110), prepared at pH = 5.5 by 3 min etching at RT (measured at  $T = 94\text{ K}$ ). The IR radiation propagates normal to the step edge as shown in the inset. The spectrum in curve (b) is obtained using s-polarized light and is enlarged by a factor of 5.

Fig. 4 summarizes the experimental evidence that the step bunching increases from (a) to (c). First, the number of lower frequency contributions around  $B_{1i}$  increases in going from (a) to (c) with the lowest frequency contributions in (c); second the coupled monohydride symmetric stretch is centered mostly at  $B_2$  in spectrum (a) and mostly at  $B_3$  in spectrum (c); third, the spectrum assigned to terrace monohydride (around  $2080\text{--}2084\text{ cm}^{-1}$ ) broadens and shifts towards lower frequencies in going from (a) to (c).

The observed splittings can be accounted for by dipole coupling. Calculations indicate that, for two steps placed next to each other, the  $B_1$  mode shifts by  $-1.35\text{ cm}^{-1}$  and the  $B_2$  mode by  $+1.60\text{ cm}^{-1}$ , relative to the frequencies of a single row of oscillators. For steps separated by one terrace row, these shifts are reduced to  $-0.60\text{ cm}^{-1}$  for  $B_1$  and  $+0.55\text{ cm}^{-1}$  for  $B_2$ . The two shoulders on either side of the two step modes:  $-0.7\text{ cm}^{-1}$  for  $B_1$  and  $+0.85\text{ cm}^{-1}$  for  $B_2$  in Fig. 4a are there-

fore consistent with monohydride steps separated by one terrace row.

In Fig. 4b, these shoulders become well-defined and increase in intensity. In particular, the feature labeled  $B_3$  becomes stronger than  $B_2$ . The shift of  $B_3$  is  $+1.70 \text{ cm}^{-1}$  with respect to  $B_2$ , suggesting that it corresponds to the symmetric stretch of neighboring monohydride steps rows, i.e., local (110) facets. Since this  $B_3$  feature is detected with s-polarization, it clearly corresponds to monohydride steps on (111) facets, oriented at  $70.3^\circ$  with respect to the original (111) surface plane. STM pictures show large scale roughness with 50–100 Å facets of non-uniform steepness on these samples, with quasi random orientation but not steep enough to be ideal (111) facets. Such observations are consistent with the formation of monohydride steps, including arrays of interacting steps.

In Fig. 4c, the  $B_3$  mode now dominates, as expected for an ideally H-terminated Si(110) surface. The complexity of the  $B_{1i}$  array in spectrum (c), however, suggests that the surface is far from being a perfectly ideally H-terminated Si(110) surface with well-ordered adjacent coupled-monohydride steps. Instead, the heterogeneity perpendicular to the monohydride step rows leads to a distribution of step-step distances and the observed  $B_{1i}$  peak positions then can be related to the individual local environments. Clearly, dipole shifts cannot account alone for the large spread of the  $B_{1i}$  modes, indicating that other contributions such as strain play a role. More extensive calculations for arrays representing specific surface topographies are therefore necessary to fully quantify the spectra and identify these strain related effects if any.

## 6. Conclusions

Chemical etching of Si(111) surfaces miscut along the  $\langle 11\bar{2} \rangle$  direction lead to macroscopic roughness (e.g. step bunching), just as for surfaces miscut along the  $\langle \bar{1}\bar{1}2 \rangle$  direction. While the monohydride-terminated steps, forming the boundaries of such facets, remain atomically straight, the step–step distances vary widely. The

degree of roughness increases with the miscut angle, and is largest in this study for the Si(110) surface. This process therefore precludes the formation an ideal, monohydride termination of the Si(110) surface with a regular array of rows. Microscopically, fluctuations in the etching process can initiate the formation of (111) facets, leading to more macroscopic roughness.

These studies help to describe the average surface morphology upon chemical etching. This is necessary to develop a comprehensive description of the etching mechanism for surfaces other than flat (111) surfaces. In particular, they indicate that the Si(100) may roughen upon chemical etching, with the formation of (111) facets. The atomic imperfection of the starting surface and different etching rates of different step structures may in fact account for the observed roughness upon etching. STM studies of the corresponding surfaces would be invaluable to develop a more refined picture of the preferential etching mechanism.

## Acknowledgements

The authors are grateful to Krishnan Raghavachari for constant and stimulating discussions and for the help with dipole calculations. P.J. gratefully acknowledges the financial support of the Deutsche Forschungsgemeinschaft (DFG).

## References

- [1] G.S. Higashi, Y.J. Chabal, G.W. Trucks and K. Raghavachari, *Appl. Phys. Lett.* 56 (1990) 656.
- [2] G.S. Higashi, R.S. Becker, Y.J. Chabal and A.J. Becker, *Appl. Phys. Lett.* 58 (1991) 1656.
- [3] P. Guyot-Sionnest, P. Dumas, Y.J. Chabal and G.S. Higashi, *Phys. Rev. Lett.* 64 (1990) 2156; P. Guyot-Sionnest, *Phys. Rev. Lett.* 66 (1991) 1489; P. Guyot-Sionnest, *Phys. Rev. Lett.* 67 (1991) 2323; M. Morin, P. Jakob, N.J. Levinos, Y.J. Chabal and A.L. Harris, *J. Chem. Phys.* 96 (1992) 6203; P. Jakob, P. Dumas and Y.J. Chabal, *Appl. Phys.* 59 (1991) 2968; S. Bouzidi, F. Coletti, J.M. Debever, P.A. Thiry, P. Dumas and Y.J. Chabal, *Phys. Rev. B* 45 (1992) 1187; K. Hricovini, R. Günther, P. Thiry, A. Taleb-Ibrahimi, G.

- Indlekofer, J.E. Bonnet, P. Dumas, Y. Petroff, X. Blase, X. Zhu, S.G. Louie, Y.J. Chabal and P.A. Thiry, *Phys. Rev. Lett.* 70 (1993) 1992;  
G.W. Trucks, K. Raghavachari, G.S. Higashi and Y.J. Chabal, *Phys. Rev. Lett.* 65 (1990) 504.
- [4] P. Jakob and Y.J. Chabal, *J. Chem. Phys.* 95 (1991) 2897.
- [5] P. Jakob, Y.J. Chabal, K. Raghavachari, R.S. Becker and A.J. Becker, *Surf. Sci.* 275 (1992) 407.
- [6] H.E. Hessel, A. Feltz, M. Reiter, U. Memmert and R.J. Behm, *Chem. Phys. Lett.* 186 (1991) 275.
- [7] (a) P. Dumas and Y.J. Chabal, *Chem. Phys. Lett.* 181 (1991) 537.  
(b) J.E. Rowe, P. Jakob, P. Dumas and Y.J. Chabal, to be published.
- [8] K. Raghavachari, P. Jakob and Y.J. Chabal, *Chem. Phys. Lett.* 206 (1993) 156.
- [9] P. Dumas, Y.J. Chabal and P. Jakob, *Appl. Surf. Sci.* 65/66 (1993) 580;  
P. Jakob and Y.J. Chabal, unpublished results.
- [10] P. Dumas, Y.J. Chabal and G.S. Higashi, *Phys. Rev. Lett.* 65 (1991) 1124.
- [11] P. Jakob, Y.J. Chabal and K. Raghavachari, *Chem. Phys. Lett.* 187 (1991) 325.
- [12] P. Jakob, Y.J. Chabal, K. Raghavachari and S.B. Christman, *Phys. Rev. B* 47 (1993) 6839.
- [13] P. Jakob, Y.J. Chabal and K. Raghavachari, *J. Electron Spectrosc. Relat. Phenom.*, in press.
- [14] G.D. Mahan and A.A. Lucas, *J. Chem. Phys.* 68 (1978) 1344.
- [15] R.S. Sorbello, *Phys. Rev. B* 32 (1985) 6294.